Design and Perception of a Soft Shape Change Beneath a Smartwatch

Zhuzhi Fan, Alexis Sanson, Thomas Rames, Céline Coutrix

Design and Perception of a Soft Shape Change Beneath a Smartwatch

ZHUZHI FAN*, CNRS, Université Grenoble Alpes, France
ALEXIS SANSON*, CNRS, Grenoble-INP, France
THOMAS RAMES, Université Grenoble Alpes, France
CÉLINE COUTRIX, CNRS, Université Grenoble Alpes, France

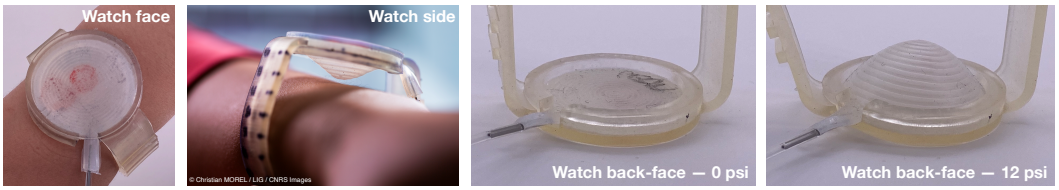

Fig. 1. We present a novel haptic notification mechanism for soft watches, through the change of curvature and contact area of its back surface. The second picture (watch side) shows a loosely tied bracelet for illustration purpose, unlike our experiment.

We explore the design of a watch that can deliver notifications through shape changes, with a specific focus on changes in curvature at the back of the watch face. We explain our design choices and the challenges we faced while creating such a watch. We conducted an experimental study to determine the absolute detection threshold (ADT) of this novel form of feedback. We compared the ADT of two different watches, both of which have a back face that can change its curvature and make contact with the wearer's wrist to notify them. These two watches exhibit different shapes when inflated with high air pressure. To determine the ADT, we conducted a standard two-down, one-up adaptive staircase procedure. Our findings show that an ADT of 3.86 psi is required to inflate the back surface for detection by participants. Overall, our qualitative findings indicate that participants enjoyed this novel type of feedback and could feel different sensations with each watch.[1]

CCS Concepts: • **Human-centered computing** → **Empirical studies in HCI**; **Haptic devices**; **Empirical studies in ubiquitous and mobile computing**; **Mobile devices**.

Additional Key Words and Phrases: Human-computer interaction, Tangible interaction, Shape-changing interfaces, Curvature-changing interfaces, Contact area, Wearable interfaces, Soft interfaces, Pneumatic actuation, Smartwatch, Notification, Haptic feedback.

*Both authors contributed equally to this research.
[1]This paper is a revised translation of a paper published in French in March 2024 [20].

Authors' Contact Information: Zhuzhi Fan, zhuzhi.fan@univ-grenoble-alpes.fr, CNRS, Université Grenoble Alpes, France; Alexis Sanson, alexis.sanson@grenoble-inp.org, CNRS, Grenoble-INP, France; Thomas Rames, thomasrames.uga@gmail.com, Université Grenoble Alpes, France; Céline Coutrix, Celine.Coutrix@cnrs.fr, CNRS, Université Grenoble Alpes, France.

ACM 2573-0142/2024/9-ART250
https://doi.org/10.1145/3676495

ACM Reference Format:
Zhuzhi Fan, Alexis Sanson, Thomas Rames, and Céline Coutrix. 2024. Design and Perception of a Soft Shape Change Beneath a Smartwatch. *Proc. ACM Hum.-Comput. Interact.* 8, MHCI, Article 250 (September 2024), 23 pages. https://doi.org/10.1145/3676495

1 Introduction

Wearing shape-changing interfaces on one's body has become a way to provide haptic and visual experiences (e.g., [57]). In particular, shape-changing notifications were found to be missed less often than vibrations [14]. As soft & shape-changing technologies are now increasingly being studied for wearable UIs (e.g., [32, 38, 42, 47, 81]), it is now very timely to experimentally study their opportunities for one of the most likely body locations –the wrist [98]– and one of the most important uses of smartwatches –notifications [2]. In addition, users like to associate very noticeable modalities to important notifications [66], and for this reason, it is important to know how noticeable these new modalities are.

Among all types of shape-change [59], curvature change is one of the most common [59]. The research question we address in this paper is to know **what is the optimum maximum curvature for users to most notice soft shape-change on their wrist?** While prior work studied (1) noticeability on the wrist of many modalities, (2) shape-change on the wrist, (3) noticeability of shape-change, and (4) tactile perception of soft and curved surfaces, none of these prior work has studied the impact of the curvature for users to notice soft shape-change on their wrists.

To answer this research question, a grand challenge lies in the isolation of parameters [3]. In particular, we need to control the maximum curvature, while keeping the watch size constant. Prior pneumatically actuated prototypes –based on simple air chambers– cannot keep the watch size constant in order to vary the maximum curvature. In order to control the curvature of the back of the watch face, we use in this paper recent advances from material sciences: baromorph materials [83]. Baromorphs are silicone surfaces embedding air channels (Figure 1). The arrangement of the channels defines the deformation of the surface when inflated.

This paper makes the following contributions:

(1) We are the first to **fabricate a wrist-worn baromorph surface** as small as ⌀42 mm and 3 mm-thin,
(2) We measure its **absolute detection threshold (ADT) on the posterior side of the wrist at 3.86 psi** –i.e. before the surface starts curving,
(3) We show that **participants felt different sensations for each maximum curvature.**

2 Related work

We position our work (Figures 2 and 3) to the following research areas: (1) noticeability studies on the wrist, (2) shape-change on the wrist, (3) perception of shape change, and more particularly of curvature change, and (4) impact of curvature and softness on the tactile experience.

2.1 Noticeability on the wrist

Notifications on the wrist are already common on smartwatches. Most research and industrial wrist-worn systems deliver vibrotactile feedback, e.g., [15, 70]. As an example, Graham-Knight et al. studied the use of vibrations on a smartwatch for non-visual communication for intimate people [37]. Vibrotactile feedback on the wrist was shown to increase speakers' awareness of time, help the coordination between a speaker and her session chair, and reduced distraction [90].

Visual notifications were also studied. E.g., Kao et al. studied the perception of on-skin visual notifications in social contexts [56]. Pohl et al. explored indirect illumination on the wrist as a way to provide notifications to users [73]. Vibrotactile and visual feedback have also been combined.

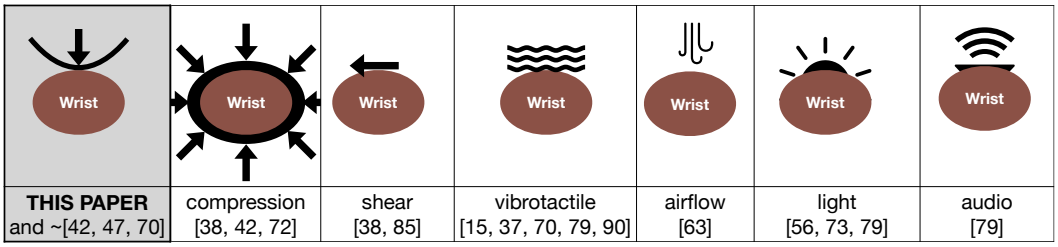

THIS PAPER and ~[42, 47, 70]	compression [38, 42, 72]	shear [38, 85]	vibrotactile [15, 37, 70, 79, 90]	airflow [63]	light [56, 73, 79]	audio [79]

Fig. 2. Positioning to prior wrist-worn feedback: we explore curvature change, while prior work explored different types of feedback.

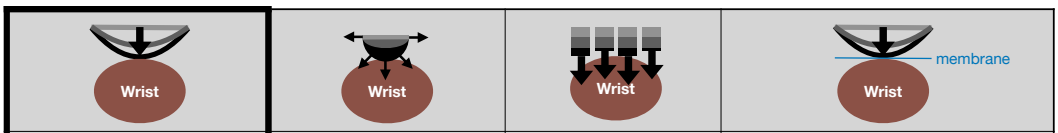

THIS PAPER	PneuHaptic [42]	RetroShape [47]	Haptic wristwatch [70]
Anisotropic deformation		×	×
Continuous surface	×		×
Soft surface	×		×
Low voltage	×	×	
High amplitude	×	×	
Temporary contact		×	

Fig. 3. Positioning to prior curvature-changing wrist-worn devices: PneuHaptic's airbag deforms in the same way in all directions (isotropic deformation), making the curvature linked to the diameter of the airbag. In addition, it is always in contact with the users' wrist [42]. RetroShape provides low curvature resolution through its discrete 4 × 4 surface and its surface is made of hard material [47]. The eyes-free haptic wristwatch relies on a membrane that is always in contact with the user's wrist, requires high voltage (up to 160V compared to our 12V) and provides limited maximum amplitude (a few mm compared to our >15mm) [70].

E.g., Schäfer et al. studied visual (light), audio, and haptic (vibration) notifications on the wrist to monitor questions and feedback during online presentations [79]. Further modalities have been studied to provide notifications to users on their wrists. E.g., Lee and Lee studied the absolute detection threshold of airflow on the wrist [63].

Stronger push on users' skin has been studied for notification. E.g., HapticClench [38] uses shape-memory alloys to provide a squeezing sensation around the arm, and InContact [85] compares pinch, squeeze, and twist sensations to vibrotactile feedback for mediated social touch. However, both provide shear force feedback on the skin, in addition to feedback perpendicular to the skin that we study here. In addition, these devices do not use curvature for haptic feedback as we do.

PneuHaptic [42] pneumatically & independently actuates five silicone chambers worn around the arm. In an informal evaluation, the authors show the effectiveness of PneuHaptic. However, the curvature of the inflated silicone chambers is fixed by their size (isotropic deformation, Figure 3). In addition, chambers are always in contact with the users' skin. On the contrary, in this paper, we propose to explore the impact of *two different curvatures* temporarily touching the skin on the absolute detection threshold, for the *same watch size*.

2.2 Shape-change on the wrist

Shape change on the wrist has been studied. E.g., Doppio [81] explores the design space of a modular screen for smartwatches. WristOrigami explores the design space for foldable multi-display smartwatches [99]. On the contrary, in this paper, we explore a more organic and soft design providing surface continuity and study the noticeability of its curvature change.

Cito [32] explores movements of the watch face, namely orbiting the face around the wrist, translating it out of the sleeve, rotating it around its orthogonal axis, tilting it, and raising it. While rising, it provides the same kind of haptic feedback that we study here, but it does not allow to vary the curvature of the watch face.

AmbienBeat [11] sticks electromagnets on silicone membranes to provide users with haptic feedback with the repulsion and attraction force of electromagnets. The authors find that haptic feedback from ambienBeat can better guide users' heart rate regulation comparing with auditory and visual guidance. However, they do not explore the feedback from surfaces with different curvatures.

RetroShape [47] provides a 2.5D shape-display on the back side of a smartwatch. The authors study the impact of the resolution of the 2.5D display on the illusion of the presence of virtual objects. The shape display that we provide is different as it is soft and continuous (Figure 3).

A haptic wristwatch [70] was proposed, where a piezoelectric disc on the back side of a watch changes curvature to hit a membrane in contact with the users' skin. However, Pasquero et al.'s change of curvature does not change the contact area on the users' skin as we do and requires higher voltage while providing lower amplitude of shape-change (Figure 3).

2.3 Perception of shape-change

Prior work studied the noticeability of shape change. E.g., Lee et al. studied visual notifications provided through a shape-changing plant [64]. Among other kinds of shape change, the authors study the change in the plant's curvature. However, its absolute visual detection threshold has not been studied. Bending a flat panel has also been studied as a way to provide visual notifications from the users' environment [54]. Authors found that such feedback in the users' near periphery was efficient and not distracting. However, these prior works study ambient notifications.

Closer to the users' bodies, different types of shape-changing notifications were studied in a video-based study [71]. In particular, around 82% of their participants said they would attend to curvature-based notifications. MorePhone [31] provides notifications by bending the whole mobile phone or its corners independently. Authors found that bending the whole phone was rather matched to urgent notifications. Leveraging the haptic information provided by the change of shape, Hoggan et al. studied if users can distinguish mobile shape-changing textures [43] at the surface of a mobile phone. On the contrary, this paper investigates the noticeability of curvature change on the wrist. Dimitriadis and Alexander studied if different types of shape-changing mobile phones were noticeable in the front pocket of trousers [14]. However, it is hard to generalize these results to another body part (wrist vs. tight) and to different types of shape-change.

Prior work studied more particularly curvature-changing interfaces (e.g., [10, 30, 40, 75]). E.g., HapTag [10] provides haptic feedback through the deformation of a thin surface located on users' skin. However, this prior work did not study the impact of the curvature of the surface on noticeability. Pneumatibles [30] decreases the air pressure step-by-step in a "detents" pattern. The authors studied users' recognition precision with different combinations of the number of detents and the initial maximum pressure in the button. However, they did not study the combination of participants' absolute detection threshold and curvature of a wrist-worn device.

2.4 Touch, curvature, and softness

Touch between a system and users can happen actively or passively. Active touch happens when users initiate the touch, e.g., when users voluntarily touch their capacitive screen. Passive touch happens when users are touched without controlling the movement, e.g., for haptic notifications.

When actively touching, humans can distinguish with their index finger a curved surface –with a base-to-peak height of 0.09 mm– from a flat surface [35]. Fan and Coutrix later studied the just-noticeable difference in curvature in different softness conditions [18]. They did not, however, study the absolute detection threshold on the wrist for passive touch. Hu and Hoffman explored round and spiky bumps on a robot skin for emotional expression [44–46]. However, they do not explore if these shapes can be used as any other type of feedback.

Other work on active touch studied perception when users slide their finger over the surface to explore the curvature [74]. However, active touch perception does not involve the same perception mechanisms as passive touch, i.e. when receiving a notification [18]. Users only use cutaneous cues[2] when passively touched. On the contrary, active touch [28] involves kinesthetic cues[2] [62].

When being passively touched on their index finger, humans judge stimuli slightly less curved than they actually are when the contact force increases (e.g., from 0.196 N to 0.588 N) [33]. In addition, humans' discrimination threshold slightly decreases when the contact area increases [34]. While contact force and area play a role when being notified through curvature change, both the effect of contact force [33] and contact area [34] are much smaller than the effect of the surface curvature itself. For this reason and for the sake of simplicity, we present our exploration around the exploration of the surface curvature to provide notification feedback, although we are aware that the resulting contact area and force play a role.

Actively touching *soft* objects, like passive touch, involves cutaneous cues. The contact area of a finger with another soft surface increases as the finger presses deeper into the surface [52]. The softer the surface, the more rapidly this contact area increases. Leveraging this phenomenon, Bicchi et al. proposed the Contact Area Spread Rate (CASR) device [6, 80]. Through the contact area between the finger and the device, this device provides users with cutaneous information. The hard device can vary its contact area with the user's finger pad through telescopic concentric cylinders. The finger presses at the top of the device and indents the cylinders more deeply. When the finger comes in contact with larger cylinders, the contact area increases. Bicchi et al. adapt the speed of the enlargement of the contact area according to the softness of the simulated surface: the softer the simulated surface, the more rapidly the contact area increases. The authors found that with this simulation, users recognize the softness almost as well as with real objects: 75% with CASR vs. 87% with real objects. This shows the important role of cutaneous cues, in particular the contact area, in softness perception. In this paper, users are *passively* touched by a soft surface. Depending on its curvature, we expect the contact area to vary. Therefore, we expect cutaneous cues to play a major role in the detection of the notification.

While prior work explored areas close to the problem addressed in this paper, this section shows that no prior work studied the absolute detection threshold of the soft curvature-changing back-face of a watch. In addition, the work closest to ours use different technologies, e.g., either confounding maximum curvature and size [42], with low curvature resolution [47], or with limited maximum curvature [70].

[2]The cutaneous cues refer to the responses of mechanoreceptors [53] innervating the finger pad skin within and in the neighborhood of the contact area [62, 87]. Kinesthetic cues refer to the sense of position and motion of limbs, along with associated forces, conveyed by the sensory receptors in the skin around the joints, joint capsules, tedons and muscles [62, 87].

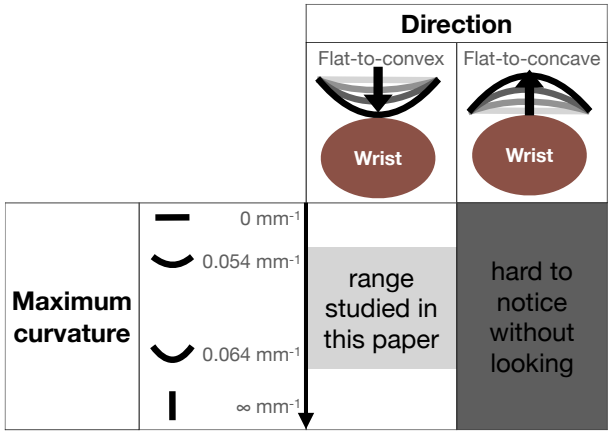

Fig. 4. Design space of the maximum curvature.

3 Watch design

To design our watch, we considered the following parameters: shape change, temporal pattern, and location.

Shape-change. Among the many possible features for shape change, such as porosity, modularity, or size [59, 76], we choose to first focus in this paper on curvature (Figure 4), as this is one of the most common changes of shape studied in the literature. We leave for future work the full exploration of the space for alternative shape change, and particularly focus on the range of curvature that a surface can offer. In order to limit the number of experimental variables for this first experiment, we chose the same curvature all around the surface (rotational symmetry).

We considered concave and convex curvatures (Figure 4). We explored in a pilot study flat-to-concave curvatures –away from the wrist as shown in Figure 4. It was hardly noticeable without looking at the wrist. For this reason, we only consider flat-to-convex deformation –towards the wrist. We then considered a range of maximum curvatures from round to spiky. We discarded extremely spiky curvatures for user safety, as even a low pressure on the skin can hurt if the contact area is extremely small [49]. As shown in Figure 4, the spikiest prototype we could fabricate offers a maximum curvature of 0.064 mm^{-1}. We then fabricated an intermediate prototype, less spiky but able to touch the skin when inflated, with a maximum curvature from 0.054 mm^{-1}.

Temporal pattern. Kinetic parameters of the change of shape, such as speed, path and direction [76], open a large design space for notifications through shape-change. Such patterns are often studied for other notification mechanisms such as vibration, e.g., [37]. In this paper, we study a simple ramp pattern: the surface linearly goes from flat to curvy, stays constantly curvy for a certain amount of time, and then linearly goes back to flat at the same speed as before.

Location. We considered alternative locations for the curvature-changing surfaces, all around the watch (Figure 5). The outside of the watch –watch face and outer bracelet in Figure 5(a)– allows for visual feedback, while the inside of the watch –watch back-face and inner bracelet in Figure 5(a)– allows for haptic feedback as it contacts with the skin. We also considered the different sides of the wrist (Figure 5(b)): posterior, medial, anterior, and lateral sides of the wrist. We only explore the watch back-face for the study presented in this paper (Figure 1) based on the following rationale: As prior work already studied the visual feedback provided by the change of curvature very close

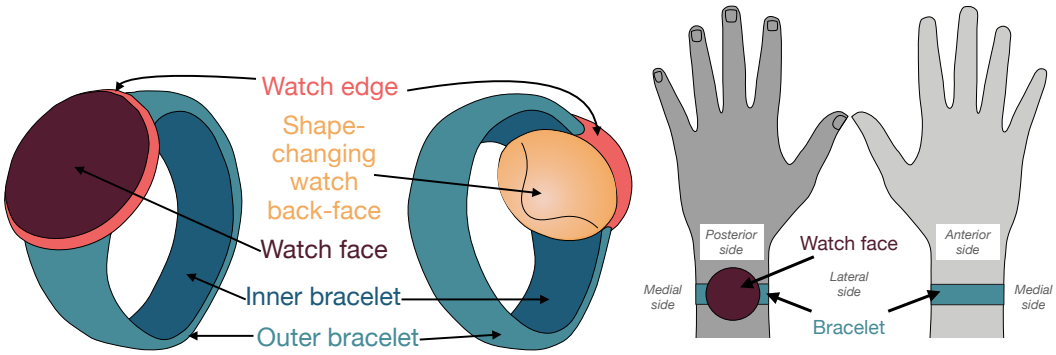

(a) Alternative shape-changing areas.

(b) Placement of a watch on the left wrist.

Fig. 5. Location design space, on the watch (left) and on the wrist (right).

to the users' wrist [54], we choose in this paper to focus on the haptic feedback provided by the change of curvature, i.e. the inner side of the watch. As the posterior side of the forearm is the most sensitive side of the forearm [17], we choose to start with the back-face of the watch (yellow in Figure 5(a)), rather than the other sides of the wrist.

To fabricate a soft, round surface that changes curvature on the back face of a watch, we leverage previous work in material sciences on soft shape-changing materials [83], namely silicone surfaces with embedded air channels called baromorphs (Figure 1). The arrangement of air channels defines the surface deformation when inflated. The distinguishing characteristic of different designs is the local curvature of the resulting inflated material: varying arrangements of air channels show different local curvatures under the same inner pressure. We focus in this paper on rotation-invariant arrangements of air channels (Figure 6) which allows us to explore the different maximum curvature (and resulting contact areas and pressure) when inflated. This material is the single one we found that allows the deformation of a continuous, soft surface in a single direction, with low voltage (12V) and >1cm amplitude of shape-change (Figure 2).

4 Watch fabrication

We are the first to fabricate such small baromorph surfaces. Making small prototypes is a grand challenge in shape-changing research and an essential step to leverage results from material science for wearable interaction [3]. We faced the three following challenges when fabricating our ⌀42 mm and 3 mm-thick baromorph surface following Siéfert et al.'s instructions made for larger surfaces [84].

3D printing a small and high-resolution mold. To precisely control the shape of a ⌀42 mm and 3 mm-thick baromorph, the challenge lies in achieving a high density of air channels in such a limited volume. We used a Form3 high precision Stereolithography (SLA) 3D printer [22] and faced a printing precision challenge and a cleaning challenge. The printer precision and the resin we used were bottlenecks to achieve thin air channels. When cleaning with isopropyl alcohol [23] in FormWash [21] after printing, the mold slightly deforms. At this scale, such fabrication defects lead to relatively large unwanted deformation of the inflated surface. To solve these problems, we systematically tried to print the molds for 0.1 mm- to 1 mm-wide air channels with the 3D printer. We tried to print with Formlabs General Purpose black, white, and clear resins [24] and noticed that the clear resin worked best. We also noticed that changing the isopropyl alcohol [23] in the

FormWash [21] more often than required by the manufacturer, prevented any residue at the surface of the mold. The smallest air channels whose mold was of sufficient quality to achieve the designed deformation were 0.4 mm wide.

Removing air bubbles trapped in the uncured silicone. As the inner structure of our baromorph is very thin, even one small air bubble inside the baromorph will lead to strong local deformation around the bubble and thus lead to an unpredicted shape when inflating the baromorph. To solve this problem when molding the silicone, we carefully remove all entrapped air inside the mixture of silicone after pouring the silicone into the mold. To do this, we vacuum degas the mixture for 3 minutes and use a needle to bring bubbles entrapped in the mold to the surface.

Gluing the cover to the channels. To complete the baromorph fabrication, we unmold the baromorph, and we spread and cure a 0.4 mm-thin silicone membrane for the cover. When gluing such a thin membrane on top of such thin and low channels, the risk lies in obstructing the 0.6mm-high channels. Air channels that are obstructed by the glue or not perfectly glued to the cover lead to relatively large unwanted deformation of the inflated surface. To solve this problem, we use the Sil-Poxy glue [86] instead of silicone [83]. The higher viscosity of the glue enables a more precise control of the thickness. We use a high precision film casting knife [8] to precisely control the thickness of the glue [86] to 0.3 mm, which is thick enough to strongly glue all inner structures but thin enough to avoid the obstruction of channels.

We tested different silicone (Smooth On Ecoflex and Dragon Skin silicone series [48]) in a pilot: Shore 00-10, Shore 00-50, Shore A-10, Shore A-20, and Shore A-30. We selected the Shore A-10 silicone, as it provided a trade-off between large shape-changing ability, and fast curing and fabrication.

We 3D print the watch case and bracelet with Formlabs Flexible 50A Resin [24] with the same printer [22].

To actuate the change of shape at the back of the watch, we developed a Python script that controls three 12 V two-way peristaltic air pumps [36] connected in parallel to inflate and deflate the shape-changing surface. The pumps are connected directly to the shape-changing surface with a long and thin Flexible PVC Tube [92] (1.5 m long, 0.8 mm inner diameter and 2.4 mm outer diameter). Through this technical design, the shape-changing surface can rapidly increase its inner pressure from 0 psi to 12 psi within 1 second.

We paid particular attention to the parameters of the proportional–integral–derivative (PID) controller in the software, to avoid the tingling sensation that we noticed during early testing. We share all the necessary materials to fabricate our prototype, including 3D models and Python scripts with the parameters of the PID controller.

5 Absolute detection threshold

The absolute detection threshold is an important and fundamental initial psychophysical measurement [27] that defines the threshold at which users can notice the feedback from the backside of the watch. Rather than measuring human sensitivity, the aim of our experiment is to determine a baseline when triggering the notification. This measure is necessary to design future interfaces and applications with the soft curvature-changing back face. We conducted this study in the lab with no distractions, to identify the baseline notification. First, determining the ADT with no distraction is a standard procedure in prior work, e.g., [5, 38, 72]. To reduce unintentional false positive inflation of results [25], we registered the experiment before collecting the data [19].

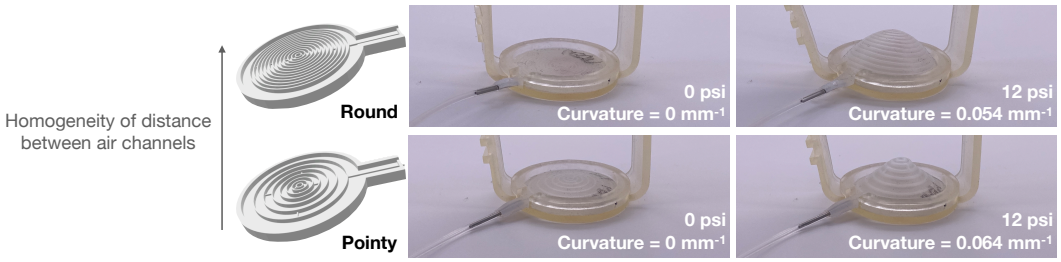

Fig. 6. Design of the molds for the surface we compare, and corresponding shape-changing watch upside down, showing the inside shape at different pressures and the corresponding measured curvatures. The molds are then 3D printed, the shape-changing surfaces are molded in silicone, and the bracelet is 3D printed using elastic resin (see section 4).

5.1 Experimental design

We conduct a within-subject experiment to find the absolute threshold at which users notice the haptic feedback provided by the watch. Participants experience two different designs of shape-change (Figure 6).

Independent variable. We vary the *homogeneity of the distance* between air channels as shown in Figure 6 in order to compare the two following MAXIMUM CURVATURES:

- **R:** The flat-to-round surface has dense and regularly spaced air channels (Figure 6, top). With baromorphs of ⌀42 mm, we find that this design results at 12 psi in the curvature of 0.054 mm^{-1}, i.e. a curvature radius of 18.52 mm (Annex A).
- **P:** The flat-to-pointy surface has air channels far from each other at the periphery and air channels close to each other at the center (Figure 6, bottom). With baromorphs of ⌀42 mm, we find that this design results at 12 psi in the curvature at the top of 0.064 mm^{-1}, i.e. a curvature radius of 15.53 mm (Annex A).

We measured experimentally the curvature of our prototypes in the range of 1-13 psi. We explain our procedure in details in Annex A. In the range of 1-10 psi, curvatures are very similar as shown in Figures 10(b) and 10(c) in Annex A. In the range of 10-13 psi, the center of the P surface is curvier than the center of the R surface.

Half of the participants start the experiment with R and the other half starts with P.

Dependent variables. We collect participants' answers –whether they notice a stimulus– at each trial. We also collect their answers to an AttrakDiff questionnaire [41] for each MAXIMUM CURVATURE, their ranking of MAXIMUM CURVATURES in terms of preference and subjective detectability, and their qualitative feedback through semi-structured interviews. We chose not to collect physical data, like the pressure on the skin or the resulting indentation of the skin, because we aim to design a usable device (HCI) rather than understanding biological mechanisms (psychophysics).

5.2 Apparatus

Participants wear the bracelet shown in Figure 1, 6, and 7(a). We fabricate the prototype as explained in section 4. The watch face is a closed surface to ensure the baromorph deforms towards the participants' wrists. The experimenter kept the bracelet securely closed with tape during the experiment. We control the fit of the bracelet by measuring participants' wrist circumference (C in cm) and adjusting the bracelet length (L in cm) to this circumference following $L = 0.8 \times C + 5.8$.

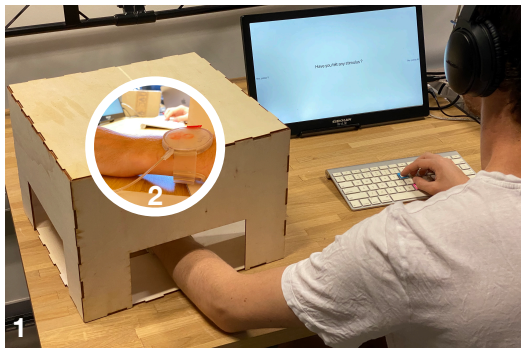

(a) (1) Overview of the experimental setup and (2) close-up of the non-dominant hand wearing the watch inside the box. The pumps and Arduino are placed in a box on a separate table on the right (cardboard box in the background in (2)).

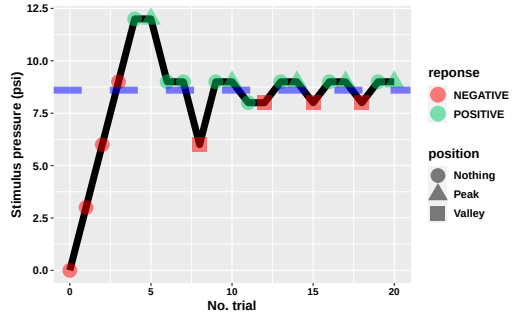

(b) Third staircase series for P9 with the flat-to-pointy surface (P). The blue dashed line shows the absolute detection threshold computed for this series.

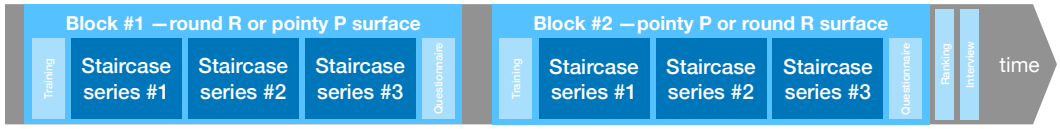

(c) Experimental timeline.

Fig. 7. Experimental setup.

To find this model, we performed a fitting pilot with 5 participants (adjusted $R^2 = 0.93$), where we made sure that the bracelet was as tight as possible while comfortable to wear.

We developed Python software to run the experiment. We provide all the necessary files to reproduce our hardware and software experimental apparatus in the supplementary material.

5.3 Participants

We recruited 12 participants from our university campus. Twelve participants allow us to test both orders of presentation of the two MAXIMUM CURVATURES. In addition, 12 participants are the most common sample size [9]. Participants were 21 to 40 years old (median = 27). Six self-reported as women and six as men. Four of them own a smartwatch providing vibrotactile feedback that they wear regularly or every day. All participants have normal sensitivity on all sides of the wrist, except P7's sensitivity on the anterior side of the wrist (Figure 5(b)) which is slightly impaired.

5.4 Procedure

Participants sit and rest their forearm at a table (Figure 7(a)). We first measure participants' wrist circumference, and sensitivity using a Semmes-Weinstein monofilament test [50] on the posterior, anterior, lateral and medial sides of the wrist (Figure 5(b)).

The experimenter installs the shape-changing watch back-face with the first MAXIMUM CURVATURE. To control a tight while comfortable fitting of the bracelet, homogeneous among participants according to the model presented in section 5.2, the experimenter closes the bracelet at the position line corresponding to participants' measured wrist circumference –black lines labeled with wrist circumferences as shown in Figure 1. We asked participants to confirm if the fitting was tight while comfortable. To isolate the haptic sensation and avoid visual feedback, participants hide their

forearm in a box as in [38, 100]. The experimenter installs the prototype inside the box around the participants' non-dominant wrist as in [38, 72, 100] (Figure 7(a)). While the dominant side is more sensitive than the non-dominant side at the mid-posterior forearm [17], testing the feedback on the non-dominant side is more ecological: most users wear their watch on the non-dominant arm [97]. In addition, to avoid any impact of the noise of the pumps, participants wear headphones playing Brownian noise.

At the beginning of each block (one for each MAXIMUM CURVATURE, Figure 7(c)), the experimenter asks participants to test the prototype, as this type of feedback is novel. To do so, the experimenter presents in a pseudo-random order either no stimulus (0 psi) or a strong stimulus (10 psi). The training stops after participants correctly judged both two zero stimuli and two strong stimuli successively[3].

We then follow a standard two-down, one-up staircase procedure [65]. In each staircase series, the first trial starts with the baromorph at 0 psi (Figure 7(b)). We maintain the desired pressure for 1s as in [63, 100]. We do not consider longer times such as 2s [38] or 5s [72] as our pilot study showed that users rather notice changes in curvature and get used to a stable curvature. We then decrease the pressure to 0 psi before participants report whether they felt any stimulus by pressing the corresponding key on a keyboard (Figure 7(a)). This is the standard procedure for non-distracted absolute detection threshold experiments [38, 63, 72, 100].

As shown in Figure 7(b), if participants do not feel any stimulus, we increase the target pressure of the next trial by a constant step of 3 psi. If participants feel the stimulus, we keep the same target pressure for the next trial. If participants feel a stimulus twice in a row, the target pressure of the next trial is reduced by the same constant step.

The increase/decrease steps are equal and constant before each reversal[4] [65]. Between the third and the fourth reversals, we decrease the step value to 1 psi to improve threshold accuracy [38, 100]. The staircase series ends after nine reversals [38]. We later compute the threshold as the mean of the last five reversals [38].

Participants take a break after each staircase series (Figure 7(c)). We repeat each staircase series three times for each MAXIMUM CURVATURE to further improve the accuracy. Thus, we collect 2 MAXIMUM CURVATURE × 3 repetitions × 12 participants = 72 measurements of the threshold.

At the end of each block, participants fill an AttrakDiff questionnaire [41]. At the end of the experiment, they rank the prototypes in terms of preference and subjective detectability. We then conduct a semi-structured interview to collect participants' qualitative feedback. The topics planned in our interview guide were the location and descriptions of the sensations, if users felt any difference between experimental conditions, and if they had any strategy to answer the perception question. The experiment lasts around 60 min for each participant.

5.5 Data analysis

From participants' answers, we compute the absolute detection threshold as the mean of the last five reversals –as in, e.g., [38, 72, 100]. We report to computed thresholds in psi –that can be converted to bar or kPa as in [100] and to mm^{-1} (Annex A). We use estimation techniques based on geometric means. Figures between brackets show 95% bootstrapped confidence intervals (CI) as recommended [16]. We use pairwise differences to show effect sizes. These methods are recommended by the APA [4] and largely adopted (e.g., [12, 13, 18, 51, 58, 61, 68]). Rather than the dichotomous inference supported by p-values, we opted for this more nuanced analysis of the

[3]Most participants succeeded in training in the first 4 trials with both 2 zero stimuli and 2 strong stimuli. Only 3 participants needed slightly more trials for training with the pointy surface, i.e., 5 trials for P5 and P11 and 7 trials for P10.
[4]A reversal is a change in direction, i.e. a local extremum shown as a triangle (peak) or a square (valley) in Figure 7(a).

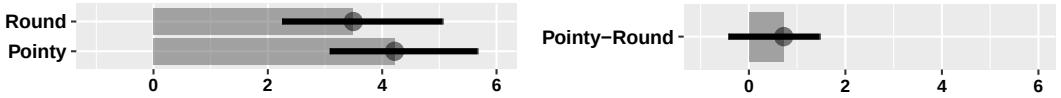

(a) Absolute detection threshold (in psi) for R and P surfaces. (b) Pairwise difference of the absolute detection thresholds (in psi).

Fig. 8. Analysis of the absolute detection thresholds. Error bars indicate bootstrapped 95% confidence intervals.

direction and magnitude of the effect. A p-value-approach reading of the results presented in this paper can be done by comparing the CIs spacing with common p-value spacing, as shown in Figure 3 in [60]. A pairwise difference is an intra-subject measurement that expresses the effect size and is computed between each of the geometric means.

We analyzed the interviews' transcripts using thematic analysis [77]. We chose thematic analysis to find out participants' experiences from our interview transcripts. Our research question was *What are users' experience with the wristwatch?* We combined inductive and deductive approaches to analyse the transcripts: While, e.g., location and sensation were topics that we questioned explicitly during interviews (deductive approach), we analyse their subthemes through an inductive approach (bottom-up from participants own words). In addition, we adopted a semantic approach, i.e. we analyzed the explicit content of the transcripts, and did not rely on assumptions underlying the data. We followed the six steps of thematic analysis:

(1) **Familiarization**: we first transcribed the audio and read thoroughly the resulting transcripts.
(2) **Coding**: we thoroughly coded all the data using the taguette software. We highlighted and labeled/coded everything we found potentially interesting regarding participants' experience with the watch.
(3) **Generating themes**: we then looked over all the codes previously defined, and grouped them into themes.
(4) **Reviewing themes**: we then read the transcripts again and analyzed if the generated themes were accurately and relevant representing the data. This lead us to readjust some of our coding.
(5) **Naming themes**: we finally reviewed the naming of each theme to make sure each precisely pictures the data.

5.6 Results

5.6.1 Absolute detection threshold. Figure 8 presents the absolute detection threshold. Figure 8(a) shows that the flat-to-round (R) surface has an average absolute detection threshold of 3.49 psi ([2.25, 5.07]), and that the flat-to-pointy (P) surface has an average absolute detection threshold of 4.22 psi ([3.11, 5.65]). Although the P surface has a slightly higher absolute detection threshold (M = +0.72 [-0.44, 1.46]) than the R surface (Figure 8(b)), the difference is very small, and the 95% confidence interval crosses 0, meaning that the actual difference might even be a little reverse. When looking at each surface at such low pressures (< 10 psi, Figure 10(c) in Annex A), we find no curvature difference between the top center of R and P surfaces.

To conclude, the MAXIMUM CURVATURE of the surface has very little to no impact *on the absolute detection threshold.* Overall, this notification modality has a low absolute detection threshold (M = 3.86 psi [2.96, 4.91]).

5.6.2 Pragmatic and Hedonic Qualities. Figure 9 presents the AttrakDiff questionnaire results [41]. An interface rated as neutral lies in the range [-1, 1], while [-3, 1] or [1, 3] denotes respectively

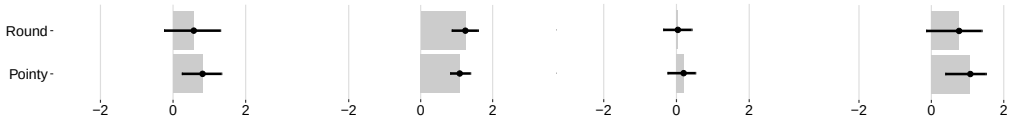

(a) Pragmatic qualities (b) Hedonic qualities (stimulation) (c) Hedonic qualities (identity) (d) Global attractivity

Fig. 9. AttrakDiff scores. Error bars indicate bootstraped 95% confidence intervals.

rather negative or positive ratings. Figure 9(a) shows that participants found both watches rather neutral in terms of usability and perceived ease of use (Pointy M=0.81 [0.24, 1.33], Round M=0.57 [-0.25, 1.30]). This can be explained by the fact that the stimulus levels were very low to measure the absolute detection threshold. Figure 9(b) shows that participants found that both watches have rather positive stimulation qualities (Pointy M=1.09 [0.82, 1.38], Round M=1.24 [0.86, 1.59]). Figure 9(c) shows that participants rated as neutral the ability of both watches to support a social function and to communicate users' identity (Pointy M=0.20 [-0.25, 0.52], Round M=0.1 [-0.36, 0.42]). Figure 9(d) shows that participants found the P surface slightly attractive (M=1.08 [0.38, 1.51]), while they found the R surface slightly more neutral (M=0.77 [-0.14, 1.39]).

5.6.3 Ranking. At the very low levels of stimuli that participants experienced in this experiment, we found no difference in the ranking of both R and P surfaces. Among 12 participants, half of the participants preferred the R surface, while the other half preferred the P surface. Seven participants think the deformation of the R surface was easier to perceive, while the other 5 participants found the contrary. As P10 mentioned that he preferred P because it was the first time he experienced this novel and pleasant stimulus, we explored if the order of presentation of each surface had an impact on the ranking and found no impact.

5.6.4 Qualitative feedback. We identified the four following main themes in the final interviews. While location, sensation and differences were themes that we asked explicitly during the interviews (top-down) while their subthemes were bottom-up (participants own words), enjoyment was a theme that emerged during our bottom-up thematic analysis.

Enjoyment. Five participants explicitly mentioned that the sensation was pleasant. For instance, P9 said that it was "very smooth, delicate", P10 said it was "soothing" and "nice", and P12 said it was "attractive". P10 said that "there's also a great deal of emotion involved". Prior work studied the relationship between shape-change and emotions [71, 89, 91]. However, these works are based on visual stimuli and not haptic ones, as in this paper. Although further work is needed to quantitatively measure how this prototype positively affects users, this positive qualitative feedback from our participants shows that this novel notification modality can be complementary to existing ones. Indeed, when comparing to their smartphones –they did not own a smartwatch– P2 and P8 mentioned that this novel type of feedback was more pleasant than vibrotactile (P2) and sound (P8) feedback.

Location of the sensations. As expected, all participants –except P9– mentioned feelings on the posterior wrist side. P1 explicitly mentioned that she felt "at the top, for the big pressures". I.e., the main sensation was at the posterior side of the wrist when the stimulus was higher than the threshold. The second most mentioned locations were the wrist lateral and medial sides. Participants could feel the very low stimuli strength that we tested during this experiment already on the sides of the wrist. As P4 said, "On the sides, I felt less, well, I had the feeling that I could feel less on

the sides". Participants mentioned less the anterior side of the wrist and for the same feeling as the lateral and medial sides. As our experiment studied very subtle stimuli, P12 even mentioned that he could feel these stimuli at the location of the cable connection. This shows that users are very sensitive to this novel type of notification modality. This is promising for future experiments exploring distracted detection threshold when users experience additional haptic sensations, like when driving a bicycle.

Description of the sensations. We found 21 subthemes describing participants' sensations from their own words: inflation (24 occurrences), deflation (15 occurrences), pressing and vibrating (14 occurrences each), touching (10 occurrences), hairs (9 occurrences), breathing (8 occurrences), squeezing (5 occurrences), spreading (3 occurrences), pricking, curvature, release, waves, moving and air blowing (2 occurrences each), massaging, sucking, tingling, pulse, skin (1 occurrence each).

The most discussed theme during interviews was inflation (9 participants). Five participants said they could feel the inflation more clearly (P4-8) than the deflation, while only one found the deflation easier to detect (P2).

The second most discussed themes were touching (P2-5, P9-11), pressing (P4, P6-7, P9, P11-12), and vibrating (P3, P4, P8, P10, P12). Participants described a local pressing sensation: "It was pressing at a point" (P7). Participants also felt the spreading of the pressure: "It really felt like it was crushing and spreading on my skin" (P11) and "it touches a corner and then spreads out" (P2).

P3-4-8 mentioned that the vibration was very subtle. P3 said "I'm in a controlled environment here, but I think that if I make everyday gestures, I might not notice the vibration". As said above, as we tested very low stimuli levels, participants could already feel the vibration before the actual change of shape.

Subjective differences between R and P surfaces. As our quantitative measurement of the ADT predicts, P1-2, P4-6, P8, and P12 mentioned that both R and P surfaces were similar during this absolute detection threshold experiment, e.g., "I had the feeling that they were the same" (P1).

However, P2-5, P7 and P11-12 were able to discuss their different sensations: "it was not the same sensation" (P11). P2 said, for instance, that "[R] must be more flat", and "with [P] you have the feeling that it touches". P4 said that "[R] had a larger surface. [P] was smaller, I think". P1 and P5 also discussed a difference in the location of their sensation: Both felt R stimulated them rather on the sides, while P stimulated them rather at the center of the posterior wrist side.

Consistently with the results of the pragmatic qualities (Figure 9(a)) and the global attractivity (Figure 9(d)), P1-4 and P10 explained during the interviews why they preferred P: "It was easier to know if I felt it" (P1), "[I found R] less detectable, and since it's less detectable, it's my least favorite." (P2), "I had more sensations with P" (P3), and "when [the stimuli] were clear, I think it was a bit clearer in P" (P4).

6 Discussion

Variance inter-participants. We found that there are differences between our participants. We made sure that all participants had normal sensitivity on the posterior side of their wrist, but we did not test their actual sensitivity threshold with a more precise Semmes-Weinstein monofilament test [50]. We hypothesize that variations in users' sensory threshold might have an impact on the ADT of this prototype. During interviews, two men (P2&11) mentioned their sensation came from hairs on the skin of the wrist: both could feel the movement before any contact with the skin because the device attracted their hair or made their hair move. Previous work [26] found that people can perceive tactile sensation with hair on their skin, e.g., perceiving the vibration of an object contacting with the hair on the dorsal part of the middle finger. Besides, in Pohl et al.'s experiment [72] measuring users' detection threshold of compression from a blood pressure

cuff on the forearm, they observed that participants with larger diameter arms have a higher detection threshold. They supposed participants' arms shape might influence the cuff's inflation characteristics. Further studies can investigate whether participants' anthropometric measurements, such as arm shape and hair on the skin, can impact users' threshold with our watch. Ecological testing of this novel notification modality should include an initial calibration in order to adapt the threshold to individual sensitivity.

Fitting of the bracelet. We paid great care to control the fitting of the bracelet (see section 5.2) so that we could reliably compare the results between participants and between blocks. However, in more ecological situations, users may fit the bracelet of their watch differently: some like to have it tightly adjusted to their wrist, while others prefer to wear it more loosely. Future work could explore the impact of the fitting of the bracelet on the detectability. As above, ecological testing of this novel notification modality should include an initial calibration in order to adapt to individual preferences, as this is already the case with vibrotactile feedback on smartwatches.

Memory effect. During interviews, three participants mentioned a possible memory effect. P1&11 mentioned that they were not sure if the sensation they had was from before or from the current stimulus. On the contrary, P4 mentioned that it was hard to remember the sensation. The impact of memory on users' haptic perception was observed in previous research [93–95]. For example, Vogels et al. found that after touching a convex (resp. concave) surface, their participants perceived a flat surface as concave (resp. convex) [95]. They also found that the memory effect can last more than 40 seconds. In another study, Gilson and Baddeley found that their participants can recall the position of a pen touching their forearm, while their remembered position precision decreases over time [29]: E.g., three seconds after been touched, the average remembered position error was measured as 15 cm. Furthermore, our experiment studied users' haptic perception on the forearm which involves hairy skin [1]. In addition to the mechanoreceptive afferents with high conduction speed (20-80 m/s) [67] that exist both in glabrous and hairy skin[5], one unique characteristic of hairy skin is the presence of C-tactile (CT) fibres, another kind of mechanoreceptive afferents with low conduction speed (0.5-2 m/s) [67], which might introduce latency in neural signal processing [96]. We could not explore the existence of a memory effect with our experimental setting. Future work should measure if there is any memory effect in order to compensate in future design, and measure the minimum interval needed between two successive stimuli to eliminate any confusion between stimuli like P1&11 mentioned.

ADT and vibrations. Our initial registered hypothesis [19] was that participants would have a lower absolute detection threshold when wearing a watch with higher maximum curvature. We therefore designed our experiment to compare curvatures. We eventually found little difference between curvatures. During the experiment, the cable coming out of the watch connects it to three pumps and does not touch the participants' skin (Figure 7(a)-2). The absolute detection threshold without distraction is so low that it might not imply shape change as shown in Figure 10(c) at 3 psi. However, we noted that the difference between curvatures is greater when the deformable surface is enclosed inside the watch (Figure 6 at 12 psi) compared to outside any enclosure (Figure 10(c) at 12 psi). Nevertheless, we believe the experimental procedure does not question the ADT we measured because we eliminated any contact with the cable and pumps (placed on another table). In fact, our prototypes feature long and thin air channels (e.g., for the rounded prototype, 664 mm long and 0.4 mm wide). Radial inflation of the channels can induce vibrations in the channels themselves due to the turbulence of the airflow [7, 69]. Therefore, these vibrations are an integral

[5]In contrast to hairy skin, glabrous skin is devoid of hairs. Glabrous skin mainly covers the palmar region of the hand and and plantar region of the feet [1].

part of the haptic modality presented. These vibrations are perceptible to our participants and come from beneath our prototype, unlike those coming from a pipe or a motor. Ultimately, we think that we cannot untie the impact of vibrations caused by the inflation, barely perceptible, and the impact of the curvature, at such a low level of stimulus needed for undistracted absolute detection.

Besides quantitative results, seven out of twelve participants explained during interviews (section 5.6.4) that they actually felt differences between round and pointy curvatures. Ultimately, our results actually tell the scientific community that this novel feedback is easily detectable, and that curvature plays little role in the *undistracted* absolute detection threshold. This does not mean that curvature will not play a role in other levels of detection, like *distracted* absolute detection threshold or just noticeable difference, as qualitative feedback showed that participants might be able to tell the difference.

Comparison. To better understand this new modality, in this study we chose to compare two alternative curvatures for the same modality. However, we have not compared this new modality to existing ones, such as those presented in Figures 2 and 3. Positioning this new modality in relation to the state of the art will be necessary in future work. In comparison, PneuHaptic [42] offers a different feedback through a series of inflatable air chambers around the arm. Their authors did not measure users' absolute detection threshold with the device. SqueezeBack [72] offers a different feedback –compression– through a blood pressure cuff applying pressure around users' forearm. Their authors measured an average detection threshold of 0.1 psi. This threshold is lower than the one we found (3.49 or 4.22 psi depending on the curvature). Designers can balance this difference with other requirements, such as multimodality, as the feedback we propose in this paper is different and relies on surface curvature change rather than compression. To further enable designers to make a decision, future work should compare users' subjective evaluation of these different haptic modalities.

Mobility. Although we have studied this new modality in the case of a connected watch, the current prototype is not mobile yet. Although the technology is not yet ready to enable this type of feedback on current watches, it is important to study the opportunities for interaction with users today [39], in parallel with technological advances such as the miniaturization of pumps.

7 Conclusion

Soft & shape-changing materials offer unprecedented opportunities for wearable UIs, in particular for notifications on the wrist. In this paper, we propose a soft curvature-changing mechanism to notify users from the back-face of their smartwatch. To do so, we use baromorph surfaces [83] to control the maximum curvature, while keeping all parameters constant, e.g. the watch size. We are the first to fabricate a baromorph surface as small as ⌀42 mm and 3 mm thin to allow for its wearability on the wrist. We conduct a standard two-down, one-up adaptive staircase procedure to find an absolute detection threshold (ADT) of 3.86 psi, i.e., the minimal pressure needed to inflate the watch to be detected by users. Our qualitative findings show that participants enjoyed this novel type of feedback, and that participants could feel different sensations with each watch.

This paper paves the way for further studies to deepen our knowledge of this novel type of feedback. *On the perception side*, now that we know the minimal detectable feedback, future work could measure users' ADT when they focus on a primary task, such as walking or cycling, and a cognitively demanding activity [38]. Future work could also measure users' just-noticeable-difference between two curvatures. In addition, prior work found that users would like to have persistent modalities for notifications [66]. Shape change could provide such persistent modalities. For this, future work needs to explore how users perceive shape change in the long term.

On the design side, future work could embed the system on the bracelet and even on the whole body, as the human sensitivity varies [17, 82], and consider other types of shape change [59]. We plan to conduct a design workshop to systematically study soft shape-changing on-skin notifications.

On the technical side, as prior work, e.g., [42, 47, 70, 78], a critical aspect for future adoption is the size of the hardware: future work should focus on miniaturizing the hardware controlling the prototype.

Acknowledgments

We thank Benoît Roman and Fablab MASTIC. This work is supported by the French National Research Agency under Grant SecondSkin (https://anr.fr/Project-ANR-21-CE33-0018), the CNRS 80 Prime under Grant MeMorI, and Université Grenoble Alpes.

References

[1] Rochelle Ackerley, Karin Saar, Francis McGlone, and Helena Backlund Wasling. 2014. Quantifying the sensory and emotional perception of touch: differences between glabrous and hairy skin. *Frontiers in behavioral neuroscience* 8 (2014), 34. https://doi.org/10.3389/fnbeh.2014.00034

[2] Neil Aitken. 2023. Most Used Features of Smartwatches. https://whatphone.com.au/guide/most-used-features-of-smartwatches/ Last retrieved: 2023-06-15.

[3] Jason Alexander, Anne Roudaut, Jürgen Steimle, Kasper Hornbæk, Miguel Bruns Alonso, Sean Follmer, and Timothy Merritt. 2018. Grand Challenges in Shape-Changing Interface Research. In *Proceedings of the 2018 CHI Conference on Human Factors in Computing Systems* (Montreal QC, Canada) *(CHI '18)*. Association for Computing Machinery, New York, NY, USA, 1–14. https://doi.org/10.1145/3173574.3173873

[4] American Psychological Association et al. 2019. *Publication Manual of the American Psychological Association, (2020)*. American Psychological Association.

[5] Olivier Bau, Ivan Poupyrev, Ali Israr, and Chris Harrison. 2010. TeslaTouch: Electrovibration for Touch Surfaces. In *Proceedings of the 23nd Annual ACM Symposium on User Interface Software and Technology* (New York, New York, USA) *(UIST '10)*. Association for Computing Machinery, New York, NY, USA, 283–292. https://doi.org/10.1145/1866029.1866074

[6] A. Bicchi, E.P. Scilingo, and D. De Rossi. 2000. Haptic discrimination of softness in teleoperation: the role of the contact area spread rate. *IEEE Transactions on Robotics and Automation* 16, 5 (2000), 496–504. https://doi.org/10.1109/70.880800

[7] W N Bond. 1931. Turbulent flow through tubes. *Proceedings of the Physical Society* 43, 1 (jan 1931), 46. https://doi.org/10.1088/0959-5309/43/1/306

[8] BYK. 2023. Film Casting Knife. https://www.byk-instruments.com/en/Physical-Properties/Paint-Application/Manual-Film-Applicators/Film-Casting-Knife/c/p-5974?variant=2328 Last retrieved July 26, 2023.

[9] Kelly Caine. 2016. Local Standards for Sample Size at CHI. In *Proceedings of the 2016 CHI Conference on Human Factors in Computing Systems* (San Jose, California, USA) *(CHI '16)*. Association for Computing Machinery, New York, NY, USA, 981–992. https://doi.org/10.1145/2858036.2858498

[10] Yanjun Chen, Xuewei Liang, Si Chen, Yuwen Chen, Hongnan Lin, Hechuan Zhang, Chutian Jiang, Feng Tian, Yu Zhang, Shanshan Yao, and Teng Han. 2022. HapTag: A Compact Actuator for Rendering Push-Button Tactility on Soft Surfaces. In *Proceedings of the 35th Annual ACM Symposium on User Interface Software and Technology* (Bend, OR, USA) *(UIST '22)*. Association for Computing Machinery, New York, NY, USA, Article 70, 11 pages. https://doi.org/10.1145/3526113.3545644

[11] Kyung Yun Choi and Hiroshi Ishii. 2020. AmbienBeat: Wrist-Worn Mobile Tactile Biofeedback for Heart Rate Rhythmic Regulation. In *Proceedings of the Fourteenth International Conference on Tangible, Embedded, and Embodied Interaction* (Sydney NSW, Australia) *(TEI '20)*. Association for Computing Machinery, New York, NY, USA, 17–30. https://doi.org/10.1145/3374920.3374938

[12] Kurtis Danyluk, Bernhard Jenny, and Wesley Willett. 2019. Look-From Camera Control for 3D Terrain Maps. In *Proceedings of the 2019 CHI Conference on Human Factors in Computing Systems* (Glasgow, Scotland Uk) *(CHI '19)*. Association for Computing Machinery, New York, NY, USA, 1–12. https://doi.org/10.1145/3290605.3300594

[13] Ruta Desai, Fraser Anderson, Justin Matejka, Stelian Coros, James McCann, George Fitzmaurice, and Tovi Grossman. 2019. Geppetto: Enabling Semantic Design of Expressive Robot Behaviors. In *Proceedings of the 2019 CHI Conference on Human Factors in Computing Systems* (Glasgow, Scotland Uk) *(CHI '19)*. Association for Computing Machinery, New York, NY, USA, 1–14. https://doi.org/10.1145/3290605.3300599

[14] Panteleimon Dimitriadis and Jason Alexander. 2014. Evaluating the Effectiveness of Physical Shape-Change for in-Pocket Mobile Device Notifications. In *Proceedings of the SIGCHI Conference on Human Factors in Computing*

Systems (Toronto, Ontario, Canada) *(CHI '14)*. Association for Computing Machinery, New York, NY, USA, 2589–2592. https://doi.org/10.1145/2556288.2557164

[15] Taylor Dixon. 2019. Good Vibrations: How Apple Dominates the Touch Feedback Game. https://www.ifixit.com/News/16768/apple-taptic-engine-haptic-feedback Last retrieved July 13, 2023.

[16] Pierre Dragicevic. 2016. Fair Statistical Communication in HCI. In *Modern Statistical Methods for HCI*. Springer, 291 – 330. https://doi.org/10.1007/978-3-319-26633-6_13

[17] Cem Erçalık and Seçil Özkurt. 2022. Two-point discrimination assessment of the upper extremities of healthy young Turkish individuals. *Turkish journal of physical medicine and rehabilitation* 68 (March 2022), 136–141. Issue 1. https://doi.org/10.5606/tftrd.2022.6263

[18] Zhuzhi Fan and Céline Coutrix. 2023. Impact of Softness on Users' Perception of Curvature for Future Soft Curvature-Changing UIs. In *Proceedings of the 2023 CHI Conference on Human Factors in Computing Systems* (Hamburg, Germany) *(CHI '23)*. Association for Computing Machinery, New York, NY, USA, Article 747, 19 pages. https://doi.org/10.1145/3544548.3581179

[19] Zhuzhi Fan, Céline Coutrix, and Alexis Sanson. 2024. Impact of surface design on the absolute detection threshold of a shape-changing back surface of a watch. https://doi.org/10.17605/OSF.IO/CQV7F

[20] Zhuzhi Fan, Alexis Sanson, Thomas Rames, and Céline Coutrix. 2024. Conception et perception d'un changement de forme molle au dos d'une montre connectée. In *Proceedings of the 35th Conference on l'Interaction Humain-Machine* (Paris, France) *(IHM '24)*. Association for Computing Machinery, New York, NY, USA, Article 8, 14 pages. https://doi.org/10.1145/3649792.3649800

[21] FormLabs. 2023. Form Wash. https://formlabs.com/post-processing/wash-cure/ Last retrieved July 25, 2023.

[22] FormLabs. 2023. Form3 high precision Stereolithography (SLA) 3D printer. https://formlabs.com/3d-printers/form-3/ Last retrieved July 25, 2023.

[23] FormLabs. 2023. Isopropyl Alcohol. https://support.formlabs.com/s/article/Isopropyl-Alcohol-IPA?language=en_US Last retrieved July 25, 2023.

[24] FormLabs. 2023. Materials. https://formlabs.com/material-selector/ Last retrieved July 25, 2023.

[25] Wolfgang Forstmeier, Eric-Jan Wagenmakers, and Timothy H. Parker. 2017. Detecting and avoiding likely false-positive findings – a practical guide. *Biological Reviews* 92 (November 2017), 1941–1968. Issue 4. https://doi.org/10.1111/brv.12315

[26] Masahiro Furukawa, Naohisa Nagaya, Yuki Hashimoto, Hiroyuki Kajimoto, and Masahiko Inami. 2009. Measurement of the detection thresholds of hair on human hairy skin using direct vibrotactile stimulation. In *World Haptics 2009 - Third Joint EuroHaptics conference and Symposium on Haptic Interfaces for Virtual Environment and Teleoperator Systems*. 127–132. https://doi.org/10.1109/WHC.2009.4810819

[27] George A Gescheider. 2016. *Psychophysics: the fundamentals* (third ed.). Routledge, Milton Park, Abingdon-on-Thames, Oxfordshire, England, UK. 46–54,183–186 pages. https://www.routledge.com/Psychophysics-The-Fundamentals/Gescheider/p/book/9781138984158

[28] James J Gibson. 1962. Observations on active touch. *Psychological review* 69, 6 (1962), 477.

[29] Elizabeth Q. Gilson and A. D. Baddeley. 1969. Tactile Short-Term Memory. *Quarterly Journal of Experimental Psychology* 21, 2 (1969), 180–184. https://doi.org/10.1080/14640746908400211 arXiv:https://doi.org/10.1080/14640746908400211

[30] Kristian Gohlke, Eva Hornecker, and Wolfgang Sattler. 2016. Pneumatibles: Exploring Soft Robotic Actuators for the Design of User Interfaces with Pneumotactile Feedback. In *Proceedings of the TEI '16: Tenth International Conference on Tangible, Embedded, and Embodied Interaction* (Eindhoven, Netherlands) *(TEI '16)*. Association for Computing Machinery, New York, NY, USA, 308–315. https://doi.org/10.1145/2839462.2839489

[31] Antonio Gomes, Andrea Nesbitt, and Roel Vertegaal. 2013. MorePhone: A Study of Actuated Shape Deformations for Flexible Thin-Film Smartphone Notifications. In *Proceedings of the SIGCHI Conference on Human Factors in Computing Systems* (Paris, France) *(CHI '13)*. Association for Computing Machinery, New York, NY, USA, 583–592. https://doi.org/10.1145/2470654.2470737

[32] Jun Gong, Lan Li, Daniel Vogel, and Xing-Dong Yang. 2017. Cito: An Actuated Smartwatch for Extended Interactions. In *Proceedings of the 2017 CHI Conference on Human Factors in Computing Systems* (Denver, Colorado, USA) *(CHI '17)*. Association for Computing Machinery, New York, NY, USA, 5331–5345. https://doi.org/10.1145/3025453.3025568

[33] AW Goodwin, KT John, and AH Marceglia. 1991. Tactile discrimination of curvature by humans using only cutaneous information from the fingerpads. *Experimental brain research* 86, 3 (1991), 663–672. https://doi.org/10.1007/BF00230540

[34] AW Goodwin and HE Wheat. 1992. Human tactile discrimination of curvature when contact area with the skin remains constant. *Experimental brain research* 88, 2 (1992), 447–450. https://doi.org/10.1007/BF02259120

[35] Ian E Gordon and Victoria Morison. 1982. The haptic perception of curvature. *Perception & psychophysics* 31, 5 (1982), 446–450. https://doi.org/10.3758/BF03204854

[36] Goso. 2023. Peristaltic Pump. https://www.amazon.fr/dp/B079GRP174/ref=pe_3044141_189395771_TE_3p_dp_1 Last retrieved July 29, 2023.

Authors' copy

[37] John Brandon Graham-Knight, Jon Michael Robert Corbett, Patricia Lasserre, Hai-Ning Liang, and Khalad Hasan. 2021. Exploring Haptic Feedback for Common Message Notification Between Intimate Couples with Smartwatches. In *Proceedings of the 32nd Australian Conference on Human-Computer Interaction* (Sydney, NSW, Australia) *(OzCHI '20)*. Association for Computing Machinery, New York, NY, USA, 245–252. https://doi.org/10.1145/3441000.3441012

[38] Aakar Gupta, Antony Albert Raj Irudayaraj, and Ravin Balakrishnan. 2017. HapticClench: Investigating Squeeze Sensations Using Memory Alloys. In *Proceedings of the 30th Annual ACM Symposium on User Interface Software and Technology* (Québec City, QC, Canada) *(UIST '17)*. Association for Computing Machinery, New York, NY, USA, 109–117. https://doi.org/10.1145/3126594.3126598

[39] Chris Harrison. 2018. The HCI Innovator's Dilemma. *Interactions* 25, 6 (Oct. 2018), 26–33. https://doi.org/10.1145/3274564

[40] Chris Harrison and Scott E. Hudson. 2009. Providing Dynamically Changeable Physical Buttons on a Visual Display. In *Proceedings of the SIGCHI Conference on Human Factors in Computing Systems* (Boston, MA, USA) *(CHI '09)*. Association for Computing Machinery, New York, NY, USA, 299–308. https://doi.org/10.1145/1518701.1518749

[41] Marc Hassenzahl. 2005. *The Thing and I: Understanding the Relationship between User and Product.* Kluwer Academic Publishers, USA, 31–42.

[42] Liang He, Cheng Xu, Ding Xu, and Ryan Brill. 2015. PneuHaptic: Delivering Haptic Cues with a Pneumatic Armband. In *Proceedings of the 2015 ACM International Symposium on Wearable Computers* (Osaka, Japan) *(ISWC '15)*. Association for Computing Machinery, New York, NY, USA, 47–48. https://doi.org/10.1145/2802083.2802091

[43] Eve Hoggan, Yi-Ta Hsieh, Kalle Myllymaa, Vuokko Lantz, Johan Kildal, Julian Eiler, and Giulio Jacucci. 2017. An Exploration of Mobile Shape-Changing Textures. In *Proceedings of the Eleventh International Conference on Tangible, Embedded, and Embodied Interaction* (Yokohama, Japan) *(TEI '17)*. Association for Computing Machinery, New York, NY, USA, 275–282. https://doi.org/10.1145/3024969.3024983

[44] Yuhan Hu and Guy Hoffman. 2020. Using Skin Texture Change to Design Emotion Expression in Social Robots. In *Proceedings of the 14th ACM/IEEE International Conference on Human-Robot Interaction* (Daegu, Republic of Korea) *(HRI '19)*. IEEE Press, 2–10.

[45] Yuhan Hu and Guy Hoffman. 2023. What Can a Robot's Skin Be? Designing Texture-Changing Skin for Human–Robot Social Interaction. *J. Hum.-Robot Interact.* 12, 2, Article 26 (apr 2023), 19 pages. https://doi.org/10.1145/3532772

[46] Yuhan Hu, Isabel Neto, Jin Ryu, Ali Shtarbanov, Hugo Nicolau, Ana Paiva, and Guy Hoffman. 2022. Touchibo: Multimodal Texture-Changing Robotic Platform for Shared Human Experiences. In *Adjunct Proceedings of the 35th Annual ACM Symposium on User Interface Software and Technology* (Bend, OR, USA) *(UIST '22 Adjunct)*. Association for Computing Machinery, New York, NY, USA, Article 68, 3 pages. https://doi.org/10.1145/3526114.3558643

[47] Da-Yuan Huang, Ruizhen Guo, Jun Gong, Jingxian Wang, John Graham, De-Nian Yang, and Xing-Dong Yang. 2017. RetroShape: Leveraging Rear-Surface Shape Displays for 2.5D Interaction on Smartwatches. In *Proceedings of the 30th Annual ACM Symposium on User Interface Software and Technology* (Québec City, QC, Canada) *(UIST '17)*. Association for Computing Machinery, New York, NY, USA, 539–551. https://doi.org/10.1145/3126594.3126610

[48] Smooth On Inc. [n. d.]. https://www.smooth-on.com/products/dragon-skin-10-nv/ Last retrieved July 24, 2023.

[49] ISO/DIS 10218-1 2018. *Robotics — Safety requirements for robot systems in an industrial environment — Part 1: Robots.* Standard. International Organization for Standardization, Geneva, CH.

[50] Jamar. 2023. Semmes-Weinstein monofilmanent sensory tests. https://www.performancehealth.com/jamar-monofilaments Last retrieved July 29, 2023.

[51] Yvonne Jansen, Jonas Schjerlund, and Kasper Hornbæk. 2019. Effects of Locomotion and Visual Overview on Spatial Memory When Interacting with Wall Displays. In *Proceedings of the 2019 CHI Conference on Human Factors in Computing Systems* (Glasgow, Scotland Uk) *(CHI '19)*. Association for Computing Machinery, New York, NY, USA, 1–12. https://doi.org/10.1145/3290605.3300521

[52] K. L. Johnson. 1985. *Normal contact of elastic solids – Hertz theory.* Cambridge University Press, Cambridge, United Kingdom, 84–106. https://doi.org/10.1017/CBO9781139171731.005

[53] Kenneth O Johnson. 2001. The roles and functions of cutaneous mechanoreceptors. *Current Opinion in Neurobiology* 11, 4 (2001), 455–461. https://doi.org/10.1016/S0959-4388(00)00234-8

[54] Lee Jones, John McClelland, Phonesavanh Thongsouksanoumane, and Audrey Girouard. 2017. Ambient Notifications with Shape Changing Circuits in Peripheral Locations. In *Proceedings of the 2017 ACM International Conference on Interactive Surfaces and Spaces* (Brighton, United Kingdom) *(ISS '17)*. Association for Computing Machinery, New York, NY, USA, 405–408. https://doi.org/10.1145/3132272.3132291

[55] Kenichi Kanatani and Prasanna Rangarajan. 2011. Hyper least squares fitting of circles and ellipses. *Computational Statistics & Data Analysis* 55, 6 (2011), 2197–2208. https://doi.org/10.1016/j.csda.2010.12.012

[56] Cindy Hsin-Liu (Cindy) Kao, Min-Wei Hung, Ximeng Zhang, Po-Chun Huang, and Chuang-Wen You. 2021. Probing User Perceptions of On-Skin Notification Displays. *Proc. ACM Hum.-Comput. Interact.* 4, CSCW3, Article 244 (jan 2021), 20 pages. https://doi.org/10.1145/3432943

Authors' copy

[57] Pavel Karpashevich, Pedro Sanches, Rachael Garrett, Yoav Luft, Kelsey Cotton, Vasiliki Tsaknaki, and Kristina Höök. 2022. Touching Our Breathing through Shape-Change: Monster, Organic Other, or Twisted Mirror. *ACM Trans. Comput.-Hum. Interact.* 29, 3, Article 22 (feb 2022), 40 pages. https://doi.org/10.1145/3490498

[58] Elio Keddisseh, Marcos Serrano, and Emmanuel Dubois. 2021. *KeyTch: Combining the Keyboard with a Touchscreen for Rapid Command Selection on Toolbars.* Association for Computing Machinery, New York, NY, USA. https://doi.org/10.1145/3411764.3445288

[59] Hyunyoung Kim, Celine Coutrix, and Anne Roudaut. 2018. Morphees+: Studying Everyday Reconfigurable Objects for the Design and Taxonomy of Reconfigurable UIs. In *Proceedings of the 2018 CHI Conference on Human Factors in Computing Systems* (Montreal QC, Canada) *(CHI '18)*. Association for Computing Machinery, New York, NY, USA, 1–14. https://doi.org/10.1145/3173574.3174193

[60] Martin Krzywinski and Naomi Altman. 2013. Error bars: The meaning of error bars is often misinterpreted, as is the statistical significance of their overlap. *Nature Methods* 10 (2013), 921 – 922. Issue 10. https://doi.org/10.1038/nmeth.2659

[61] Caitlin Kuhlman, Diana Doherty, Malika Nurbekova, Goutham Deva, Zarni Phyo, Paul-Henry Schoenhagen, MaryAnn VanValkenburg, Elke Rundensteiner, and Lane Harrison. 2019. Evaluating Preference Collection Methods for Interactive Ranking Analytics. In *Proceedings of the 2019 CHI Conference on Human Factors in Computing Systems* (Glasgow, Scotland Uk) *(CHI '19)*. Association for Computing Machinery, New York, NY, USA, 1–11. https://doi.org/10.1145/3290605.3300742

[62] Susan J Lederman and Roberta L Klatzky. 2009. Haptic perception: A tutorial. *Attention, Perception, & Psychophysics* 71, 7 (2009), 1439–1459. https://doi.org/10.3758/APP.71.7.1439

[63] Jaeyeon Lee and Geehyuk Lee. 2016. Designing a Non-Contact Wearable Tactile Display Using Airflows. In *Proceedings of the 29th Annual Symposium on User Interface Software and Technology* (Tokyo, Japan) *(UIST '16)*. Association for Computing Machinery, New York, NY, USA, 183–194. https://doi.org/10.1145/2984511.2984583

[64] Jarrett G.W. Lee, Bongshin Lee, and Eun Kyoung Choe. 2023. Decorative, Evocative, and Uncanny: Reactions on Ambient-to-Disruptive Health Notifications via Plant-Mimicking Shape-Changing Interfaces. In *Proceedings of the 2023 CHI Conference on Human Factors in Computing Systems* (Hamburg, Germany) *(CHI '23)*. Association for Computing Machinery, New York, NY, USA, Article 320, 16 pages. https://doi.org/10.1145/3544548.3581486

[65] H. Levitt. 2005. Transformed Up-Down Methods in Psychoacoustics. *The Journal of the Acoustical Society of America* 49, 2B (08 2005), 467–477. https://doi.org/10.1121/1.1912375 arXiv:https://pubs.aip.org/asa/jasa/article-pdf/49/2B/467/12184369/467_1_online.pdf

[66] Afra Mashhadi, Akhil Mathur, and Fahim Kawsar. 2014. The Myth of Subtle Notifications. In *Proceedings of the 2014 ACM International Joint Conference on Pervasive and Ubiquitous Computing: Adjunct Publication* (Seattle, Washington) *(UbiComp '14 Adjunct)*. Association for Computing Machinery, New York, NY, USA, 111–114. https://doi.org/10.1145/2638728.2638759

[67] Francis McGlone, Johan Wessberg, and Håkan Olausson. 2014. Discriminative and Affective Touch: Sensing and Feeling. *Neuron* 82, 4 (2014), 737–755. https://doi.org/10.1016/j.neuron.2014.05.001

[68] Pranathi Mylavarapu, Adil Yalcin, Xan Gregg, and Niklas Elmqvist. 2019. Ranked-List Visualization: A Graphical Perception Study. In *Proceedings of the 2019 CHI Conference on Human Factors in Computing Systems* (Glasgow, Scotland Uk) *(CHI '19)*. Association for Computing Machinery, New York, NY, USA, 1–12. https://doi.org/10.1145/3290605.3300422

[69] R. Neelamegam and V. Shankar. 2015. Experimental study of the instability of laminar flow in a tube with deformable walls. *Physics of Fluids* 27, 2 (02 2015), 024102. https://doi.org/10.1063/1.4907246 arXiv:https://pubs.aip.org/aip/pof/article-pdf/doi/10.1063/1.4907246/14843752/024102_1_online.pdf

[70] Jerome Pasquero, Scott J. Stobbe, and Noel Stonehouse. 2011. A Haptic Wristwatch for Eyes-Free Interactions. In *Proceedings of the SIGCHI Conference on Human Factors in Computing Systems* (Vancouver, BC, Canada) *(CHI '11)*. Association for Computing Machinery, New York, NY, USA, 3257–3266. https://doi.org/10.1145/1978942.1979425

[71] Esben W. Pedersen, Sriram Subramanian, and Kasper Hornbæk. 2014. Is My Phone Alive? A Large-Scale Study of Shape Change in Handheld Devices Using Videos. In *Proceedings of the SIGCHI Conference on Human Factors in Computing Systems* (Toronto, Ontario, Canada) *(CHI '14)*. Association for Computing Machinery, New York, NY, USA, 2579–2588. https://doi.org/10.1145/2556288.2557018

[72] Henning Pohl, Peter Brandes, Hung Ngo Quang, and Michael Rohs. 2017. Squeezeback: Pneumatic Compression for Notifications. In *Proceedings of the 2017 CHI Conference on Human Factors in Computing Systems* (Denver, Colorado, USA) *(CHI '17)*. Association for Computing Machinery, New York, NY, USA, 5318–5330. https://doi.org/10.1145/3025453.3025526

[73] Henning Pohl, Justyna Medrek, and Michael Rohs. 2016. ScatterWatch: Subtle Notifications via Indirect Illumination Scattered in the Skin. In *Proceedings of the 18th International Conference on Human-Computer Interaction with Mobile Devices and Services* (Florence, Italy) *(MobileHCI '16)*. Association for Computing Machinery, New York, NY, USA,

7–16. https://doi.org/10.1145/2935334.2935351

[74] Sylvia C Pont, Astrid ML Kappers, and Jan J Koenderink. 1999. Similar mechanisms underlie curvature comparison by static and dynamic touch. *Perception & Psychophysics* 61, 5 (1999), 874–894. https://doi.org/10.3758/BF03206903

[75] Michael Raitor, Julie M. Walker, Allison M. Okamura, and Heather Culbertson. 2017. WRAP: Wearable, restricted-aperture pneumatics for haptic guidance. In *2017 IEEE International Conference on Robotics and Automation (ICRA)*. 427–432. https://doi.org/10.1109/ICRA.2017.7989055

[76] Majken K. Rasmussen, Esben W. Pedersen, Marianne G. Petersen, and Kasper Hornbæk. 2012. Shape-Changing Interfaces: A Review of the Design Space and Open Research Questions. In *Proceedings of the SIGCHI Conference on Human Factors in Computing Systems* (Austin, Texas, USA) *(CHI '12)*. Association for Computing Machinery, New York, NY, USA, 735–744. https://doi.org/10.1145/2207676.2207781

[77] Sage (Ed.). 2022. *Thematic analysis: A practical guide*.

[78] Aryan Saini, Rakesh Patibanda, Nathalie Overdevest, Elise Van Den Hoven, and Florian 'Floyd' Mueller. 2024. PneuMa: Designing Pneumatic Bodily Extensions for Supporting Movement in Everyday Life. In *Proceedings of the Eighteenth International Conference on Tangible, Embedded, and Embodied Interaction* (<conf-loc>, <city>Cork</city>, <country>Ireland</country>, </conf-loc>) *(TEI '24)*. Association for Computing Machinery, New York, NY, USA, Article 1, 16 pages. https://doi.org/10.1145/3623509.3633349

[79] René Schäfer, Tobias Wagner, Ulyana Lavnikevich, and Jan Borchers. 2023. Enhancing Notification Awareness for Online Presenters via a Wrist-Worn Device. In *Extended Abstracts of the 2023 CHI Conference on Human Factors in Computing Systems* (Hamburg, Germany) *(CHI EA '23)*. Association for Computing Machinery, New York, NY, USA, Article 103, 6 pages. https://doi.org/10.1145/3544549.3585855

[80] Enzo Pasquale Scilingo, Matteo Bianchi, Giorgio Grioli, and Antonio Bicchi. 2010. Rendering Softness: Integration of Kinesthetic and Cutaneous Information in a Haptic Device. *IEEE Transactions on Haptics* 3, 2 (2010), 109–118. https://doi.org/10.1109/TOH.2010.2

[81] Teddy Seyed, Xing-Dong Yang, and Daniel Vogel. 2016. Doppio: A Reconfigurable Dual-Face Smartwatch for Tangible Interaction. In *Proceedings of the 2016 CHI Conference on Human Factors in Computing Systems* (San Jose, California, USA) *(CHI '16)*. Association for Computing Machinery, New York, NY, USA, 4675–4686. https://doi.org/10.1145/2858036.2858256

[82] Kannathu Shibin and Asir Samuel. 2013. The Discrimination of Two-point Touch Sense for the Upper Extremity in Indian Adults. *International Journal of Health and Rehabilitation Sciences* 2 (01 2013), 38–43.

[83] Emmanuel Siéfert, Etienne Reyssat, José Bico, and Benoît Roman. 2019. Bio-inspired pneumatic shape-morphing elastomers. *Nature materials* 18, 1 (2019), 24–28. https://doi.org/10.1038/s41563-018-0219-x

[84] Emmanuel Siefert and Benoit Roman. 2019. https://vimeo.com/420256797 Last retrieved July 13, 2023.

[85] Melanie F. Simons, Alice C. Haynes, Yan Gao, Yihua Zhu, and Jonathan Rossiter. 2020. In Contact: Pinching, Squeezing and Twisting for Mediated Social Touch. In *Extended Abstracts of the 2020 CHI Conference on Human Factors in Computing Systems* (Honolulu, HI, USA) *(CHI EA '20)*. Association for Computing Machinery, New York, NY, USA, 1–9. https://doi.org/10.1145/3334480.3382798

[86] Smooth-on. 2023. Sil Poxy Glue. https://www.smooth-on.com/products/sil-poxy/ Last retrieved July 25, 2023.

[87] M. A. Srinivasan and R. H. LaMotte. 1995. Tactual discrimination of softness. *Journal of Neurophysiology* 73, 1 (1995), 88–101. https://doi.org/10.1152/jn.1995.73.1.88 arXiv:https://doi.org/10.1152/jn.1995.73.1.88 PMID: 7714593.

[88] Andrew A. Stanley, James C. Gwilliam, and Allison M. Okamura. 2013. Haptic jamming: A deformable geometry, variable stiffness tactile display using pneumatics and particle jamming. In *2013 World Haptics Conference (WHC)*. Institute of Electrical and Electronics Engineers, Daejeon, Korea (South), 25–30. https://doi.org/10.1109/WHC.2013.6548379

[89] Paul Strohmeier, Juan Pablo Carrascal, Bernard Cheng, Margaret Meban, and Roel Vertegaal. 2016. An Evaluation of Shape Changes for Conveying Emotions. In *Proceedings of the 2016 CHI Conference on Human Factors in Computing Systems* (San Jose, California, USA) *(CHI '16)*. Association for Computing Machinery, New York, NY, USA, 3781–3792. https://doi.org/10.1145/2858036.2858537

[90] Diane Tam, Karon E. MacLean, Joanna McGrenere, and Katherine J. Kuchenbecker. 2013. The Design and Field Observation of a Haptic Notification System for Timing Awareness during Oral Presentations. In *Proceedings of the SIGCHI Conference on Human Factors in Computing Systems* (Paris, France) *(CHI '13)*. Association for Computing Machinery, New York, NY, USA, 1689–1698. https://doi.org/10.1145/2470654.2466223

[91] Haodan Tan, John Tiab, Selma Šabanović, and Kasper Hornbæk. 2016. Happy Moves, Sad Grooves: Using Theories of Biological Motion and Affect to Design Shape-Changing Interfaces. In *Proceedings of the 2016 ACM Conference on Designing Interactive Systems* (Brisbane, QLD, Australia) *(DIS '16)*. Association for Computing Machinery, New York, NY, USA, 1282–1293. https://doi.org/10.1145/2901790.2901845

[92] Saint Gobain Tygon. 2024. Flexible PVCTube. https://fr.rs-online.com/web/p/tuyaux-et-tubes-flexibles/3139454 Last retrieved May 17, 2024.

[93] Bernard J Van der Horst, Maarten JA Duijndam, Myrna FM Ketels, Martine TJM Wilbers, Sandra A Zwijsen, and Astrid ML Kappers. 2008. Intramanual and intermanual transfer of the curvature aftereffect. *Experimental Brain Research* 187 (2008), 491–496. https://doi.org/10.1007/s00221-008-1390-0

[94] Bernard J. van der Horst, Wouter P. Willebrands, and Astrid M.L. Kappers. 2008. Transfer of the curvature aftereffect in dynamic touch. *Neuropsychologia* 46, 12 (2008), 2966–2972. https://doi.org/10.1016/j.neuropsychologia.2008.06.003

[95] Ingrid M L C Vogels, Astrid M L Kappers, and Jan J Koenderink. 1996. Haptic Aftereffect of Curved Surfaces. *Perception* 25, 1 (1996), 109–119. https://doi.org/10.1068/p250109 arXiv:https://doi.org/10.1068/p250109 PMID: 8861174.

[96] Christian Weidner, Martin Schmelz, Roland Schmidt, Björn Hammarberg, Kristin Ørstavik, Marita Hilliges, H. Erik Torebjörk, and Hermann O. Handwerker. 2002. Neural Signal Processing: The Underestimated Contribution of Peripheral Human C-Fibers. *Journal of Neuroscience* 22, 15 (2002), 6704–6712. https://doi.org/10.1523/JNEUROSCI.22-15-06704.2002 arXiv:https://www.jneurosci.org/content/22/15/6704.full.pdf

[97] Hui-Shyong Yeo, Juyoung Lee, Hyung-il Kim, Aakar Gupta, Andrea Bianchi, Daniel Vogel, Hideki Koike, Woontack Woo, and Aaron Quigley. 2019. WRIST: Watch-Ring Interaction and Sensing Technique for Wrist Gestures and Macro-Micro Pointing. In *Proceedings of the 21st International Conference on Human-Computer Interaction with Mobile Devices and Services* (Taipei, Taiwan) *(MobileHCI '19)*. Association for Computing Machinery, New York, NY, USA, Article 19, 15 pages. https://doi.org/10.1145/3338286.3340130

[98] Clint Zeagler. 2017. Where to Wear It: Functional, Technical, and Social Considerations in on-Body Location for Wearable Technology 20 Years of Designing for Wearability. In *Proceedings of the 2017 ACM International Symposium on Wearable Computers* (Maui, Hawaii) *(ISWC '17)*. Association for Computing Machinery, New York, NY, USA, 150–157. https://doi.org/10.1145/3123021.3123042

[99] Kening Zhu, Morten Fjeld, and Ayça Ünlüer. 2018. WristOrigami: Exploring Foldable Design for Multi-Display Smartwatch. In *Proceedings of the 2018 Designing Interactive Systems Conference* (Hong Kong, China) *(DIS '18)*. Association for Computing Machinery, New York, NY, USA, 1207–1218. https://doi.org/10.1145/3196709.3196713

[100] Mengjia Zhu, Amirhossein H. Memar, Aakar Gupta, Majed Samad, Priyanshu Agarwal, Yon Visell, Sean J. Keller, and Nicholas Colonnese. 2020. PneuSleeve: In-Fabric Multimodal Actuation and Sensing in a Soft, Compact, and Expressive Haptic Sleeve. In *Proceedings of the 2020 CHI Conference on Human Factors in Computing Systems* (Honolulu, HI, USA) *(CHI '20)*. Association for Computing Machinery, New York, NY, USA, 1–12. https://doi.org/10.1145/3313831.3376333

A Curvature measurements

We verified the curvature of our prototypes as in [88]. We first took pictures of our prototypes (Figure 10(a)) with a Panasonic Lumix G Hybrides camera with a LUMIX G VARIO 14-140 lens (Focal length f=135 mm, resolution 1096× 2160). Pictures were calibrated to remove the distortion of the camera lens with OpenCV 4.6.0[6]. To ensure measurement accuracy, we took pictures of each prototype with each air pressure three times, by inflating them from 0 psi to objective pressure each time.

We then detected the contour of the curved surface of each stimulus with OpenCV. We fitted points to this contour (Figure 10(a)) using the circle-fit 0.1.3 [55] python package, to finally find its curvature as presented in the green square in Figure 10(a). As shown in Figure 10(c), the curvatures of our prototypes are not constant across the whole surface, so we fitted the central part where the prototype first made contact with the participants' skin for curvature calculation. We take the central ⌀15 mm part, as cropping images with smaller size leads to failed circle fitting because of too few pixels of prototypes among noise. To convert the curvature from pixels (px) to mm as shown in the y-axis of Figure 10(b), we fixed a vernier scale on the 3D printed support (Figure 10(a)) to ensure the precision of the conversion. We found that 69.9 mm on the scale equals 1213 px in the pictures. Therefore, we convert our measurements of the curvature with 0.058 mm/px. Figure 10(b) presents on the y-axis the results of our measurements with the average curvature of each prototype in each pressure condition. With Figure 10(c), we can see that when air pressure is low (i.e., R prototype under 6 psi and P prototype under 5 psi), our prototypes barely inflate and stay nearly flat. This is coherent with the poor circle fitting result shown in Figure 10(b), i.e., low

[6] https://docs.opencv.org/4.x/

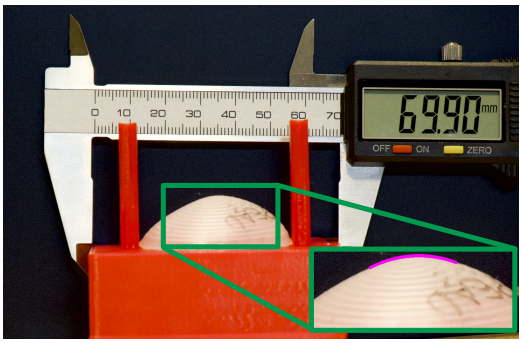

(a) Setup for curvature measurement. The fitted arc is shown in purple.

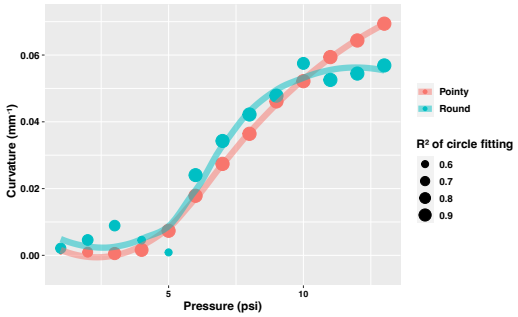

(b) Curvature measurements of each prototype inflated at different air pressures.

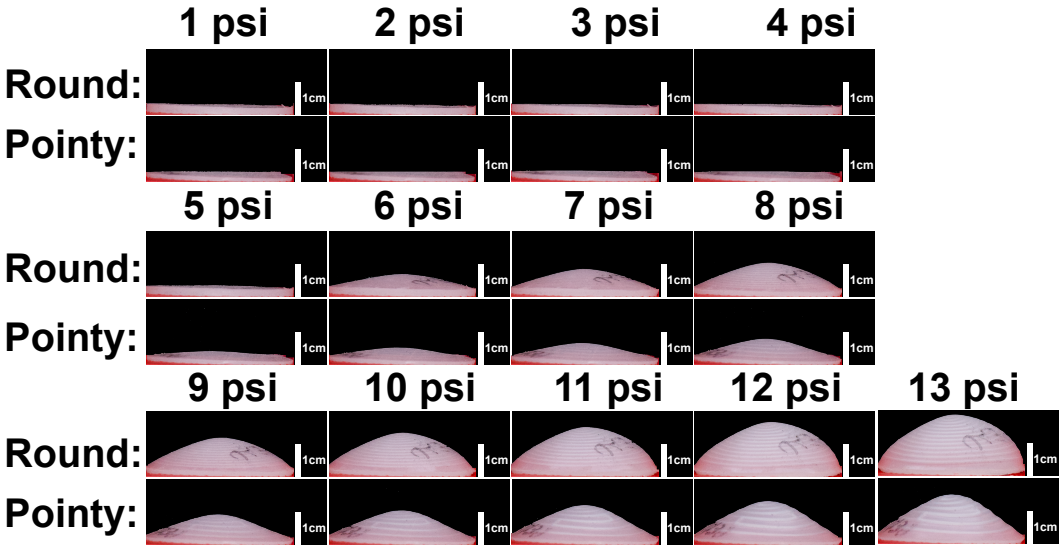

(c) Prototypes at different air pressures.

Fig. 10. Curvature measurement setup and results.

R^2 value in low-pressure conditions. The exact values in Figure 10(b) and the code to compute the curvature are available in the supplementary material.